AD-A171 051 FREQUENCY ESTIMATION BY PRINCIPAL COMPONENT AR SPECTRAL ESTIMATION METHOD..(U) RHODE ISLAND UNIV KINGSTON DEPT OF ELECTRICAL ENGINEERING S M KAY ET AL. MAY 86 1/1

UNCLASSIFIED N00014-84-K-0527 F/G 12/1 NL

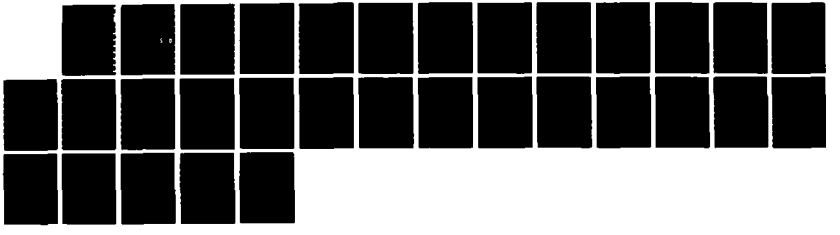

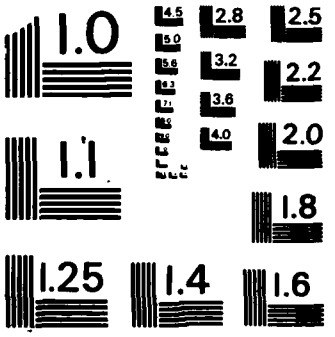

MICROCOPY RESOLUTION TEST CHART
NATIONAL BUREAU OF STANDARDS-1963-A

Report Number 4

FREQUENCY ESTIMATION BY PRINCIPAL COMPONENT AR SPECTRAL ESTIMATION METHOD WITHOUT EIGEN DECOMPOSITION

STEVEN KAY AND ARNAB SHAW

Department of Electrical Engineering
University of Rhode Island
Kingston, Rhode Island 02881

June 1986

prepared for

OFFICE OF NAVAL RESEARCH

Statistic and Probability Branch
Arlington, Virginia 22217
under Contract N00014-84-K-0527
S. M. Kay, Principal Investigator

Approved for public release; distribution unlimited

SECURITY CLASSIFICATION OF THIS PAGE (When Data Entered)

REPORT DOCUMENTATION PAGE	READ INSTRUCTIONS BEFORE COMPLETING FORM
1. REPORT NUMBER: 4	2. GOVT ACCESSION NO.: AD-A170 051
	3. RECIPIENT'S CATALOG NUMBER:
4. TITLE (and Subtitle): Frequency Estimation by Principal Component AR Spectral Estimation Method without Eigendecomposition	5. TYPE OF REPORT & PERIOD COVERED: August 1984 to July 1986
	6. PERFORMING ORG. REPORT NUMBER:
7. AUTHOR(s): Steven M. Kay and Arnab K. Shaw	8. CONTRACT OR GRANT NUMBER(s): N00014-84-0527
9. PERFORMING ORGANIZATION NAME AND ADDRESS: Electrical Engineering Department, University of Rhode Island, Kingston, Rhode Island 02881	10. PROGRAM ELEMENT, PROJECT, TASK AREA & WORK UNIT NUMBERS:
11. CONTROLLING OFFICE NAME AND ADDRESS: Office of Naval Research, Department of the Navy, Arlington, Virginia 22217	12. REPORT DATE: May 1986
	13. NUMBER OF PAGES: 25
14. MONITORING AGENCY NAME & ADDRESS (if different from Controlling Office):	15. SECURITY CLASS. (of this report): Unclassified
	15a. DECLASSIFICATION DOWNGRADING SCHEDULE:

16. DISTRIBUTION STATEMENT (of this Report)

Approved for public release. Distribution Unlimited.

17. DISTRIBUTION STATEMENT (of the abstract entered in Block 20, if different from Report)

18. SUPPLEMENTARY NOTES

19. KEY WORDS (Continue on reverse side if necessary and identify by block number)

Frequency Estimation
Spectral Estimation
High Resolution

20. ABSTRACT (Continue on reverse side if necessary and identify by block number)

For accurate frequency estimation Principal Component Autoregressive (PC-AR) spectral estimation methods have received considerable attention in the recent literature. Explicit computation of the Eigen-decomposition of the autocorrelation matrix is required to obtain the PC-AR solution. An alternative approach called the 'Eigenvalue filtering method' (EFM) where the eigenspace need not be computed, is proposed in this paper. The proposed method utilizes the geometry of the distribution of the eigenvalues

DD FORM 1 JAN 73 1473 EDITION OF 1 NOV 65 IS OBSOLETE

S/N 0102-LF-014-6601

SECURITY CLASSIFICATION OF THIS PAGE (When Data Entered)

FREQUENCY ESTIMATION BY PRINCIPAL COMPONENT AR SPECTRAL ESTIMATION METHOD WITHOUT EIGENDECOMPOSITION

Steven M. Kay and Arnab K. Shaw
Electrical Engineering Department
University Of Rhode Island
Kingston, RI 02881.

ABSTRACT

For accurate frequency estimation Principal Component Autoregressive (PC-AR) spectral estimation methods have received considerable attention in the recent literature. Explicit computation of the Eigen-decomposition of the autocorrelation matrix is required to obtain the PC-AR solution. An alternative approach called the 'Eigenvalue filtering method' (EFM) where the eigenspace need not be computed, is proposed in this paper. The proposed method utilizes the geometry of the distribution of the eigenvalues in a matrix function so that it closely approximates the pseudoinverse of the autocorrelation matrix. It is shown via computer simulation that compared with the Forward/Backward method, the proposed method enhances the threshold in SNR by about 6-8 dB. Further improvement is obtained by a simple subset selection method and a second eigenvalue filtering iteration.

Permission to publish this abstract separately is granted.

This work was supported by the Office of Naval Research under contract N00014-84-K-0527. The second author is supported by a grant from Transcom Electronics.

INTRODUCTION

Estimation of parameters of multiple sinusoidal signals imbedded in white noise is a very well researched problem in signal processing. It is also one of the fundamental problems encountered in a variety of seemingly unrelated fields, e.g, geophysics, economics, radar, astronomy, sonar, etc.. Ideas and techniques emerging from different fields have transgressed and intermingled, resulting in a certain maturity of this problem. Many researchers have reported various aspects of this problem in recent and earlier literature. Useful references are listed in Kumaresan's thesis [1] and also in a recent book by Haykin et al [2] and in the forthcoming book by Kay [3].

One of the ideas which has received considerable attention is the use of Singular Value Decomposition (SVD) of a large order (larger than number of sinusoids) autocorrelation matrix estimated from data or equivalently, the principal component analysis of the autocorrelation matrix [4]. The SVD approach produces orthogonal eigenspaces consisting of the signal subspace and the noise subspace. The many variants of SVD based frequency estimation methods that are presently available, usually make use of either the signal subspace or the noise subspace to estimate the frequency components. One disadvantage of these approaches is the burden of computing the eigenspaces explicitly. To avoid this, a different approach has been undertaken in the present work, where the knowledge of the geometry of the distribution of eigenvalues has been exploited. An appropriate function of the autocorrelation matrix is suggested to preserve the signal subspace and nullify the noise subspace. It is shown that if the geometry of the

distribution of the eigenvalues is exactly known, then the suggested matrix function eliminates the noise subspace while keeping the signal eigenvalues intact. In practical situations, however, the exact distribution of the eigenvalues will not be known. A few theorems which relate the elements of a hermitian matrix to its eigenvalues have been invoked to obtain bounds on the signal eigenvalues. Then the estimated bound (or threshold) is utilized in the proposed matrix function to remove the effects of most of the noise eigenvalues. Simulations on the same data with a large number of independent noise realizations have been performed and the results have been compared to those obtained by using the modified covariance or Forward/Backward (FB) method and the Cramer-Rao (CR) lower bound. Without computing the eigenspace explicitly, the proposed method enhances the threshold (of Signal to Noise Ratio) by about 6-8 dB over the FB method. Then a subset selection method is used which improves the threshold by 2-6 dB for the FB and the proposed methods. For the present method a second iteration is then shown to enhance the threshold further.

This paper is arranged as follows. In Section I the problem is formulated for multiple sinusoids in noise and a brief discussion of the FB method and the Principal Component Autoregressive (PC-AR) method is presented. In Section II, the proposed eigenvalue filtering method is described with theoretical analysis and simulation results. Section III consists of some concluding observations.

SECTION I : PROBLEM FORMULATION

Ia : Problem Definition

Given N samples of observation data composed of p complex sinusoids in white noise denoted by

$$x(n) = \sum_{i=1}^{p} A_i \, e^{j(2\pi f_i n + \phi_i)} + z(n) \qquad n = 0,1,\ldots,N-1 \tag{1}$$

where $A_1, A_2, \ldots, A_p$ are the amplitudes $f_1, f_2, \ldots, f_p$ are the frequencies and $\phi_1, \phi_2, \ldots, \phi_p$ are the phases associated with each sinusoid, the problem is to estimate $A_1, A_2, \ldots, A_p$, $f_1, f_2, \ldots, f_p$ and $\phi_1, \phi_2, \ldots, \phi_p$. The observation noise z(n) is assumed to be zero mean and white. Usually, the number of complex sinusoids p is known or an estimate of it is available and the phases $\phi_1, \phi_2, \ldots, \phi_p$ are assumed to be random (or fixed but unknown) and uniformly distributed between 0 and 2π.

Ib : Previous Results

The oldest and probably the most widely used frequency estimator is the periodogram. It can be shown [8] that for p = 1, periodogram maximizes the likelihood function. But for p > 1, the interaction between the frequencies causes poorer estimates except when the frequencies are far enough apart or if they are separated by K/N , where K is an integer not equal to a multiple of N. Especially, for closely spaced sinusoids, i.e. when the separation between two sinusoids is less than 1/N, then periodogram cannot resolve the two peaks and exhibits a single peak instead of two. The maximum likelihood

estimator for p greater than 1 is computationally intensive whether grid search [1] or iterative techniques [3,4] are used. High resolution spectral estimation techniques have been extensively used by many researchers to overcome the problems of the periodogram. Since the approach taken in this paper is an indirect implementation of the principal component autoregressive frequency estimator [5], a brief review of this method is in order. The proposed method is then described in Section II.

The data composed of p sinusoids as given by equation (1) may be thought of as a limiting form AR process with narrow band peaks at the p sinusoidal frequency locations. Such an AR process can be modeled as the output of an AR filter driven by white noise. With this model at hand, one can use a reasonable estimator of the autocorrelation function (ACF) from the data and then estimate the AR parameters from the following relationship,

$$\underline{a} = - \underline{R}^{-1} \underline{r} \tag{2}$$

The last equation is the solution of the following normal equations encountered in FB method.

$$\begin{bmatrix} C_{11} & C_{12} & \cdots & C_{1L} \\ C_{21} & C_{22} & \cdots & C_{2L} \\ \cdot & \cdot & \cdots & \cdot \\ \cdot & \cdot & \cdots & \cdot \\ C_{L1} & \cdots & \cdots & C_{LL} \end{bmatrix} \begin{bmatrix} a_1 \\ a_2 \\ \cdot \\ \cdot \\ a_L \end{bmatrix} = - \begin{bmatrix} C_{10} \\ C_{20} \\ \cdot \\ \cdot \\ C_{L0} \end{bmatrix} \tag{3}$$

or $\underline{R}\ \underline{a} = - \underline{r}$

where,

$$C_{ij} = \frac{1}{2(N-L)} \left[\sum_{n=L}^{N-1} x^*(n-i)\, x(n-j) + \sum_{n=0}^{N-L} x(n+i)\, x^*(n+j) \right], \quad \begin{matrix} i = 0, 1, \ldots, L \\ j = 0, 1, \ldots, L. \end{matrix}$$

are the ACF estimates used in the FB method. The frequency estimates are obtained by choosing p zeros of A(z) that are closest to the unit circle, where $A(z) = 1 + \sum a_i z^{-i}$ is known as the estimated prediction error filter (PEF). A Choice of L such that $N/3 < p < N/2$ has been shown to yield reasonably good estimates. At low SNR values (below 20 dB), the FB method fails to resolve closely spaced peaks due to the effect of noise on the ACF estimates. This problem has been alleviated to a great extent by the use of the principal component solution. In the PC-AR method, the following eigen-decomposition of the $\underline{R}$ matrix is used,

$$\underline{R} = \sum_{i=1}^{p} \lambda_i \underline{v}_i \underline{v}_i^H + \sum_{i=p+1}^{L} \lambda_i \underline{v}_i \underline{v}_i^H$$

where, $\lambda_1 \geq \lambda_2 \geq \cdots \geq \lambda_p \geq \lambda_{p+1} \geq \cdots \geq \lambda_L$ are the eigenvalues (real valued and positive, because $\underline{R}$ is hermitian and positive definite) and $\underline{v}_1, \underline{v}_2, \ldots \underline{v}_L$ are the corresponding orthonormal eigenvectors. Using this notation, the solution in (2) can now be expressed as,

$$\underline{a} = -\left[\sum_{i=1}^{p} \frac{1}{\lambda_i} \underline{v}_i \underline{v}_i^H \right] \underline{r} - \left[\sum_{i=p+1}^{L} \frac{1}{\lambda_i} \underline{v}_i \underline{v}_i^H \right] \underline{r} \qquad (4)$$

A principal component solution would omit the second term which corresponds to the L-p noise eigenvalues and retain the first term that corresponds to the p signal eigenvalues so that the PC solution is given by,

$$\underline{a}_{PC} = -\sum_{i=1}^{p} \frac{1}{\lambda_i} \underline{v}_i \underline{v}_i^H \underline{r} \tag{5}$$

Equation (5) is also written as,

$$\underline{a}_{PC} = -\underline{R}^{\#} \underline{r} \tag{6}$$

where $\underline{R}^{\#}$, which is commonly known as the pseudoinverse of $\underline{R}$, is defined as,

$$\underline{R}^{\#} = \sum_{i=1}^{p} \frac{1}{\lambda_i} \underline{v}_i \underline{v}_i^H \tag{7}$$

As an interesting interpretation of the $\underline{a}_{PC}$ solution that should be noted is that if $\underline{R}$ is singular the normal equations (3) will have infinitely many solutions out of which one unique solution that minimizes the Euclidean norm $\underline{a}^H\underline{a}$ is, in fact, the $\underline{a}_{PC}$ solution given by (6). This is also known as a 'minimum-norm' solution. For the FB case, this occurs when the order L is greater than the number of sinusoids p and no additive noise is present. Also for the noiseless FB case, the corresponding PEF A(z) has p zeros on the unit circle at the sinusoidal frequency locations and the other L-p zeros of the PEF lie inside the unit circle [1].

SECTION II : NEW METHOD

IIa : Motivation

The PC-AR solution retains the p smallest eigenvalues of $\underline{R}^{-1}$ and zeros out the L-p largest eigenvalues. This operation can be functionally represented as,

$$\underline{a}_{PC} = - f(\underline{R}^{-1})\ \underline{r} \tag{8}$$

where $f(\underline{R}^{-1})$ defines the functional operation of zeroing out the L-p largest eigenvalues of $\underline{R}^{-1}$, i.e, $f(\underline{R}^{-1}) = \underline{R}^{\#}$, where $\underline{R}^{\#}$ is defined in (7). The eigenvalues corresponding to the matrix $f(\underline{R}^{-1})$ are given by $f(\Lambda)$, where Λ denotes the eigenvalues of $\underline{R}^{-1}$ which are related to the eigenvalues of $\underline{R}$ as,

$\Lambda_1 = 1/\lambda_1$, $\Lambda_2 = 1/\lambda_2$, . . . $\Lambda_L = 1/\lambda_L$ so that $\Lambda_1 \leq \Lambda_2 \leq . . \leq \Lambda_L$

In $\underline{R}^{\#}$ as given by equation (7), all eigenvalues greater than Λ_p, i.e, the L-p largest eigenvalues are zeros which may be represented as

$$\begin{aligned} f(\Lambda) &= \Lambda \quad \text{for } \Lambda \leq \Lambda_p \\ &= 0 \quad \text{for } \Lambda > \Lambda_p \end{aligned} \tag{9}$$

Geometrically, $f(\Lambda)$ as described by equation (9), can be represented by the plot in Fig. 1. This geometry suggests that one could as well find a function $g(\Lambda)$ that closely approximates $f(\Lambda)$ of Fig. 1 and then use the corresponding matrix function $g(\underline{R}^{-1})$ in place of $\underline{R}^{\#}$ in the $\underline{a}_{PC}$ solution in equation (6). The advantage of using $g(\underline{R}^{-1})$ instead of $\underline{R}^{\#}$ is that the eigen-decomposition of $\underline{R}^{-1}$ need not be computed since $g(\underline{R}^{-1})$ has the same effect on $\underline{R}^{-1}$ as the use of $\underline{R}^{\#}$. This approach whereby a desired matrix function $f(\underline{A})$ is replaced by an easier-to-calculate matrix function $g(\underline{A})$, where $\underline{A}$ is any L x L matrix, has received some attention in numerical

analysis [7]. These techniques are based on the idea that if $g(\Lambda)$, the eigenfunction corresponding to $g(\underline{A})$, closely approximates $f(\Lambda)$ on the eigenspace of the corresponding matrix $\underline{A}$, then $f(\underline{A})$ is approximated by $g(\underline{A})$. The approximate matrix functions do not involve eigenvalues and eigenvectors, thus avoiding explicit eigen-decomposition.

IIb : Possible Approximations of $f(\Lambda)$

It can be easily shown [7] that the function $g(\underline{A})$ of an L x L matrix $\underline{A}$, has the same eigenvectors as the original matrix. Also, if Λ is any eigenvalue of the original matrix $\underline{A}$, then the corresponding eigenvalue of the matrix function $g(\underline{A})$ is simply $g(\Lambda)$. Some approximating functions are now discussed.

1) Polynomial Approximation : The coefficients of the polynomial,

$$g(\Lambda) = g_0 + g_1 \Lambda + g_2 \Lambda^2 + \ldots + g_M \Lambda^M \qquad (10)$$

can be found by a least squares fit with $f(\Lambda)$ at equally (or unequally) spaced Λ values. M may be any arbitrary integer. This approximation was attempted using IMSL Package Subroutines and also by directly programming it in Fortran. But as shown in Fig.2 for the case of M = 10, the approximations always yielded a poor fit, possibly because of the discontinuity of $f(\Lambda)$ at $\Lambda = \Lambda_0$. Also, $g(\Lambda)$ is seen to have negative going values for some regions of $\Lambda > \Lambda_0$. The effect of this may be adverse in the equivalent matrix function because negative values of $g(\Lambda)$ may result in negative eigenvalues of $g(\underline{R}^{-1})$. In such cases, the resulting matrix function will not be positive semidefinite, which is inconsistent with the property of a covariance

matrix. The frequency estimates obtained using this approximation technique were poor and hence the polynomial approximation seemed unacceptable.

2) Rational Function Approximation : The use of a rational function of Λ given by,

$$g(\Lambda) = \frac{N(\Lambda)}{D(\Lambda)} \tag{11}$$

is now examined. One choice of $g(\Lambda)$ which closely approximates $f(\Lambda)$ in (9) is given by,

$$g(\Lambda) = \frac{\Lambda}{1 + (\Lambda / \tilde{\Lambda})^M} \qquad \text{for } 0 \leq \Lambda \leq \Lambda_L \tag{12}$$

where $\tilde{\Lambda}$ is chosen such that, $\Lambda_p < \tilde{\Lambda} < \Lambda_{p+1}$. It can be easily verified that for sufficiently large M

$$g(\Lambda) \approx \Lambda \quad \text{for } \Lambda < \tilde{\Lambda}$$
$$\approx 0 \quad \text{for } \Lambda > \tilde{\Lambda}$$

In Fig. 3 $(1/\tilde{\Lambda})g(\Lambda)$ vs. $\Lambda / \tilde{\Lambda}$ is plotted. It is evident that even for small values of M, $g(\Lambda)$ dies off quickly enough for $\Lambda >> \tilde{\Lambda}$. In practical situations most of the noise eigenvalues of $\underline{R}^{-1}$ are much larger than Λ_p so that even if a low value of M is used, those noise eigenvalues will be substantially suppressed.

IIc : Analysis of the rational matrix function $g(\underline{R}^{-1})$

The matrix function corresponding to the eigenvalue function $g(\Lambda)$ in (12)

can be written as

$$g(\underline{R}^{-1}) = \underline{R}^{-1}\left[\underline{I} + \left[\frac{\underline{R}^{-1}}{\tilde{\lambda}}\right]^{M}\right]^{-1} \tag{13}$$

where $\underline{I}$ is the L x L identity matrix. It is proved that $g(\underline{R}^{-1}) \longrightarrow \underline{R}^{\#}$ as M becomes large. Since the eigenvalues of $\underline{R}^{-1}/\tilde{\lambda}$ are $\lambda_1/\tilde{\lambda}, \lambda_2/\tilde{\lambda}, \ldots, \lambda_L/\tilde{\lambda}$ and $\underline{R}^{-1}$ and $\underline{R}^{-1}/\tilde{\lambda}$ have the same set of eigenvectors $\underline{v}_1, \underline{v}_2, \ldots, \underline{v}_L$, $g(\underline{R}^{-1})$ has the following decomposition,

$$g(\underline{R}^{-1}) = \underline{V}\begin{bmatrix}\lambda_1 & & \underline{0}\\ & \lambda_2 & \\ \underline{0} & & \lambda_L\end{bmatrix}\underline{V}^{H}\left[\underline{I} + \underline{V}\begin{bmatrix}(\lambda_1/\tilde{\lambda})^{M} & & \underline{0}\\ & (\lambda_2/\tilde{\lambda})^{M} & \\ \underline{0} & & (\lambda_L/\lambda)^{M}\end{bmatrix}\underline{V}^{H}\right]^{-1}$$

where $\underline{V} = [\underline{v}_1\ \underline{v}_2 \ldots \underline{v}_L]$. Now, since $\underline{R}$ is a positive definite matrix its eigenvectors form an orthogonal set, so that, $\underline{V}\underline{V}^{H} = \underline{I}$ if the eigenvectors are normalized to have unit lengths. Since $\underline{R}^{-1}$ has the same eigenvectors as, one can write,

$$g(\underline{R}^{-1}) = \underline{V}\begin{bmatrix}\lambda_1 & & \underline{0}\\ & \lambda_2 & \\ \underline{0} & & \lambda_L\end{bmatrix}\underline{V}^{H}\underline{V}\begin{bmatrix}\left[1+(\lambda_1/\tilde{\lambda})^{M}\right]^{-1} & & \underline{0}\\ & \left[1+(\lambda_2/\tilde{\lambda})^{M}\right]^{-1} & \\ \underline{0} & & \left[1+(\lambda_L/\tilde{\lambda})^{M}\right]^{-1}\end{bmatrix}\underline{V}^{H}$$

$$= \underline{V}\begin{bmatrix}\lambda_1/(1+(\lambda_1/\tilde{\lambda})^{M}) = g(\lambda_1) & & \underline{0}\\ & \lambda_2/(1+(\lambda_2/\tilde{\lambda})^{M}) = g(\lambda_2) & \\ & & \ddots\\ \underline{0} & & \lambda_L/(1+(\lambda_L/\tilde{\lambda})^{M}) = g(\lambda_L)\end{bmatrix}\underline{V}^{H}$$

This derivation verifies the statement made in Section IIb about the eigenvalues and eigenvectors of a function of a matrix.

Now, for large enough M,

$$g(\Lambda) \longrightarrow 0 \quad \text{for } \Lambda > \bar{\Lambda} \text{ and}$$

$$\longrightarrow \Lambda \quad \text{for } \Lambda < \bar{\Lambda}$$

So we have for large M,

$$g(\underline{R}^{-1}) \longrightarrow \underline{V} \begin{bmatrix} \Lambda_1 & & & \underline{0} & \\ & \Lambda_2 & & & \\ & & \ddots & & \\ & & & \Lambda_D & \\ \underline{0} & & & & 0 \\ & & & & & 0 \\ & & & & & & 0 \end{bmatrix} \underline{V}^H = \sum_{i=1}^{D} \frac{1}{\lambda_i} \underline{v}_i \underline{v}_i^H = \underline{R}^{\#}$$

The above analysis justifies that if the proper scaling parameter $\bar{\Lambda}$ is known such that $\Lambda_D < \bar{\Lambda} < \Lambda_{D+1}$, then the suggested matrix function indeed tends to $\underline{R}^{\#}$ for large M. In practical situations, however, $\bar{\Lambda}$ will not be known unless one computes the eigenvalues explicitly, but that, in fact, was intended to be avoided in the first place. In the next section, two matrix theorems are stated to obtain a reasonable estimate of $\bar{\Lambda}$.

IId : Choice of $\bar{\Lambda}$

It is a well known fact that the trace of matrix is equal to the sum of the eigenvalues of the matrix. The noise eigenvalues $\Lambda_{D+1}, \ldots, \Lambda_L$ are much larger than the signal eigenvalues. Therefore, it can be expected that the average of the eigenvalues will be larger than Λ_D. So one choice of $\bar{\Lambda}$ is $\bar{\Lambda}'$ = (1/L) * sum of the eigenvalues of $\underline{R}^{-1}$ = (1/L) $\sum \underline{R}^{-1}(i,i)$ = (1/L) Trace($\underline{R}^{-1}$), where $\underline{R}^{-1}(i,i)$ denotes the (i,i)th element of the matrix $\underline{R}^{-1}$. Also, since $\underline{R}^{-1}$ is a hermitian matrix with eigenvalues $\Lambda_1 \leq \Lambda_2 \leq \ldots \leq \Lambda_L$,

the following fact is also true [6].

If $c_2, c_3, \ldots, c_L$ and $d_1, d_2, \ldots, d_L$ are real numbers such that,

$$d_i \geq \underline{R}^{-1}(L+1-i, L+1-i) + c_i \sum_{j > L+1-i} |\underline{R}^{-1}(L+1-i, j)|^2 \qquad i = 1, 2, \ldots, L$$

$$c_i > 0, \quad d_i - d_{i-1} \geq 1/c_i, \quad i = 2, 3, \ldots, L \tag{14}$$

then $\quad \Lambda_i \leq d_i, \quad i = 1, 2, \ldots, L$

In numerous simulation examples with large number of noise realizations, the explicit computation of the eigenvalues of $\underline{R}^{-1}$ indicated that if $c_i = 1$ for all i, i.e, if the d_i's are chosen such that

$$d_i = \underline{R}^{-1}(L+1-i, L+1-i) + \sum_{j > L+1-i} |\underline{R}^{-1}(L+1-i, j)|^2 \qquad i = 1, 2, \ldots, L,$$

then $\Lambda_i \leq d_i \ \forall i$, i.e, the eigenvalues were found to be always less than the corresponding d_i's. So the d_i's obtained from the above expression can be used as the upperbounds of the Λ_i's. For the simulation example described in the following section where p = 2 was considered, d_2 provides an upperbound for Λ_2. So another choice of $\tilde{\Lambda}$ is, $\tilde{\Lambda}'' = \underline{R}^{-1}(L-1, L-1) + |\underline{R}^{-1}(L-1, L)|^2$. Finally, $\tilde{\Lambda}$ was chosen as the smaller of the above two bounds, i.e, $\tilde{\Lambda} = \min(\tilde{\Lambda}', \tilde{\Lambda}'')$.

IIe: Simulation Results

For the process given by (1) with two sinusoids or

$$x(n) = A_1 e^{j(2\pi f_1 n + \phi_1)} + A_2 e^{j(2\pi f_2 n + \phi_2)} + z(n) \tag{15}$$

where $f_1 = 0.52$, $f_2 = 0.50$, $A_1 = 1.0$, $A_2 = 1.0$, $\phi_1 = \pi/4$ and $\phi_2 = 0$. z(n) is a computer generated, complex white gaussian noise sequence with variance $2\sigma^2$, where σ^2 is the variance of the real and imaginary parts of z(n). SNR for either sinusoid is defined as $10 \log_{10}(A_1^2/2\sigma^2)$. For every trial 25 (=N) data points were generated. This same data set was used in references [1]

and [5]. For every trial the sinusoidal signal was kept unchanged and a different realization of z(n) was generated. 500 such trials were performed for the FB method and the proposed method. The mean, variance and MSE were calculated for f_1. In Table I, bias and MSE are tabulated for different SNR values. A plot of $10\log_{10}(1/\text{MSE})$ vs. SNR is shown in Fig. 4 for the present method (plot marked EFM) and the FB method. For the FB method with L=8 which exihibited the best results, the threshold MSE occurs at about an SNR of 20 dB and for the present method with L=10 and M=6 which produced the best results, the threshold occured at 14-15 dB. As shown in Fig. 4, improved performance is obtained for L=10 and M=6 with a second eigenvalue filtering iteration which will be explained in Section IIh. The Cramer-Rao lower bound for an unbiased estimator is also tabulated in Table I and plotted in Fig. 4 for comparison.

To indicate the improvement in performance which may be obtained if λ could be more accurately determined, the threshold parameter λ was computed explicitly as $(\lambda_p + \lambda_{p+1})/2$. Then, the present method exhibited results very close to the PC-AR method when L = 12 to 16 was used with M = 4,5. The best results are obtained for L = 16 and M = 5 as seen in Fig.4.

IIf : <u>Computation of amplitudes (A_i's)</u>

Once the estimates f_1, f_2 are obtained, the complex amplitudes $A_{c1} = A_1 e^{j\phi_1}$ and $A_{c2} = A_2 e^{j\phi_2}$ are computed as the least squares solution,

$$[A_{c1}\ A_{c2}]^T = [\underline{E}_2^+\ \underline{E}_2]^{-1}\ \underline{E}_2^+\ \underline{x} \qquad (16)$$

where 'T' denotes matrix transpose and '+' denotes matrix transpose conjugated and

$$\underline{E}_2 = \begin{bmatrix} 1 & 1 \\ e^{j2\pi f_1} & e^{j2\pi f_2} \\ \vdots & \vdots \\ e^{j2\pi(N-1)f_1} & e^{j2\pi(N-1)f_2} \end{bmatrix} = \begin{bmatrix} \underline{e}_{f_1} & \underline{e}_{f_2} \end{bmatrix} \qquad (17)$$

and $\underline{x} = [\, x(0)\ x(1)\ .\ .\ .\ x(N-1)\,]^T$. The absolute values of A_{c1} and A_{c2} are used as the amplitude estimates A_1 and A_2.

IIg: Threshold enhancement by subset selection

A simple subset selection method for frequency estimates which performed well in simulations is now described. Computationally, this method is relatively less expensive than similar approaches reported earlier in [9] and [10]. Instead of choosing only 2 zeros of A(z) nearest to the unit circle, 4 zeros closest to the unit circle were chosen. The amplitudes corresponding to those 4 frequency estimates were computed from,

$$[\, A_{c1}\ A_{c2}\ A_{c3}\ A_{c4}\,]^T = [\, \underline{E}_4^+\ \underline{E}_4\,]^{-1}\ \underline{E}_4^+\ \underline{x} \qquad (18)$$

where,
$\underline{E}_4 = \begin{bmatrix} \underline{e}_{f_1} & \underline{e}_{f2} & \underline{e}_{f_3} & \underline{e}_{f_4} \end{bmatrix}$, and the $\underline{e}_{f_i}$'s are similarly defined as in (17).

Then the frequencies corresponding to the two largest amplitude estimates were used as frequency estimates. The results of subset selection approach are plotted in Fig.5. Compared to the case of choosing the frequency estimates from the two zeros closest to the unit circle, about 2-3 dB threshold enhancement is observed. EFM was used for L=8 and M=15 in both the cases. For the case of p sinusoids, 2p zeros of A(z) closest to the unit

circle would produce 2p amplitude estimates, out of which the frequency estimates should be chosen corresponding to the p largest amplitudes. Simulation experience indicates that instead of 2p zeros, if even more zeros closest to the unit circle are picked to estimate the largest p amplitudes, further threshold enhancement may be obtained. Using L = 8 and M = 15, the best results were obtained when the two frequencies had been chosen in the same manner from the six zeros of A(z) closest to the unit circle. As shown in Fig. 5, about 3 dB further threshold enhancement is observed.

IIh : Threshold Enhancement by a Second iteration

The choice of λ as described in section IId leaves a few noise eigenvalues unchanged in the approximating matrix function $g(\underline{R}^{-1})$ because the λ chosen according to those bounds is usually larger than a few eigenvalues which are greater than λ_p. In the second iteration, one can eliminate a few more noise eigenvalues from $g(\underline{R}^{-1})$ following the same procedure as in the first iteration. λ should be chosen as the average of the diagonal elements of $g(\underline{R}^{-1})$, because the first iteration reduces most of the noise eigenvalues, causing the average eigenvalue to be decreased. In the second iteration, the new matrix function can again be obtained from equation (13) where R^{-1} should be replaced by $g(\underline{R}^{-1})$ and the new λ should be used for scaling. The best results were obtained for L = 10 and M = 6. The results are plotted in Fig. 4 along with the previous results. This second iteration reduces the MSE so that the plot is closer to the CR bound line and the threshold also decreases by 2-3dB. The subset selection method suggested in the section IIg provided further enhancement of this threshold. The best results were

obtained for L = 12 and M = 4, as shown in Fig. 5. The plots show the results of two cases. For the first case, the two frequencies having the two largest amplitudes were chosen out of the six zeros of A(z) closest to the unit circle, whereas for the second case, eight zeros closest to the unit circle were used to obtain the two frequency estimates. As seen in Fig. 5., the second case yielded the best performance compared to the Cramer-Rao bounds and the known λ case.

SECTION III: OBSERVATIONS AND CONCLUSIONS

It has been shown that if λ is known exactly, the proposed eigenvalue filtering method works almost as well as the Principal Component based frequency estimation method. If λ is estimated from the covariance matrix, an improvement of 5-6 dB in the threshold is obtained over the Forward/Backward method. Additional threshold enhancement of about 6-7 dB can be obtained with a second iteration at the cost of more computation. A PEF order $L \approx N/3$ was observed to yield the best results when only the first iteration was used. A possible reason for this may be that for $L < N/3$, the signal eigenvalues are too noise corrupted while for $L > N/3$, the eigenvalue filtering method preserves too many noise eigenvalues. A better choice of λ should enhance the threshold at least to that of the Principal Component based techniques. A simple subset selection method has also been suggested to improve the threshold for the Forward/Backward and the proposed methods.

REFERENCES

1) R. Kumaresan. "Estimating The Parameters of Exponentially Damped or Undamped Sinusoidal Signals in Noise". PhD Disseration, Electrical Engineering Department, University of Rhode Island, 1982.

2) S. Haykin et. al., Array Signal Processing, Prentice Hall, Englewood Cliffs, 1985.

3) S. M. Kay, Modern Spectral Estimation: Theory and Application, To be Published by Prentice-Hall.

4) R. Kumaresan and A. K. Shaw, "High Resolution Bearing Estimation Without Eigendecomposition", IEEE Proceedinds of ICASSP 1985, vol.2, pp. 576-579.

5) D. W. Tufts and R. Kumaresan, "Estimation of frequencies of Multiple Sinusoids: Making Linear Prediction Perform Like Maximum Likelihood", IEEE Proceedings, vol.70, pp. 975-989, Sept. 1982.

6) M. Marcus and H. Ming, A Survey Of Matrix Theory And Matrix Inequalities, Allyn & Bacon Inc., 1964.

7) G. H. Golub and C. F. VanLoan, Matrix Computations, The Johns Hookins University Press, pp. 380-403, 1983.

8) D. C. Rife and R. R. Boorstyn, "Single Tone Parameter Estimation from Discrete Time Observations.", IEEE Transaction on Information Theory, Vol. IT-20, pp.591-598, Sept. 1974.

9) R. Kumaresan,D. W. Tufts and L. L. Scharf, "A Prony Method for Noisy Data : Choosing the Signal Components and Selecting the Order in Exponential Signal Models", IEEE Proceedings, vol.72, No.2, pp.230-233, February 1984.

10) R. R. Hocking and L. L. Leslie, "Selection of the Best Subset in Regression Analysis", Technometrics, Vol.9, pp. 537-540, 1967.

SNR in dB	BIAS	MSE	CR BOUND
30.0	0.1924×10^{-4}	0.193×10^{-6}	0.967×10^{-7}
20.0	0.1179×10^{-3}	0.197×10^{-5}	0.968×10^{-6}
15.0	0.1620×10^{-3}	0.970×10^{-5}	0.306×10^{-5}
12.0	0.6969×10^{-2}	0.195×10^{-2}	0.762×10^{-5}
10.0	0.1485×10^{-1}	0.432×10^{-2}	0.967×10^{-5}
5.0	0.8570×10^{-1}	0.278×10^{-1}	0.306×10^{-4}

TABLE 1 : BIAS and MSE for the estimate of f_1 (= 0.52) using Eigenfiltering method. Cramer-Rao bounds are also listed. 500 different noise realizat--ions were used at each SNR.

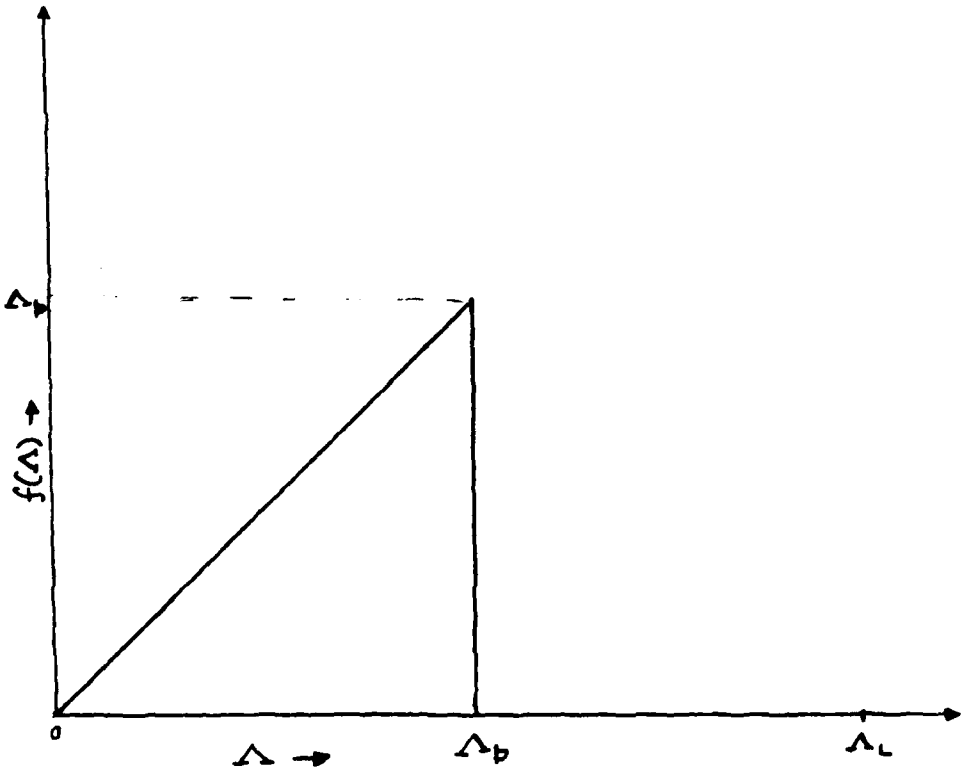

Fig. 1. Geometric representation of the distribution of the eigenvalues of the pseudoinverse of $\underline{R}$. The plot depicts that the pseudoinverse retains only the signal eigenvalues $\Lambda_1, \ldots, \Lambda_p$ and sets the rest of the eigenvalues to zero .

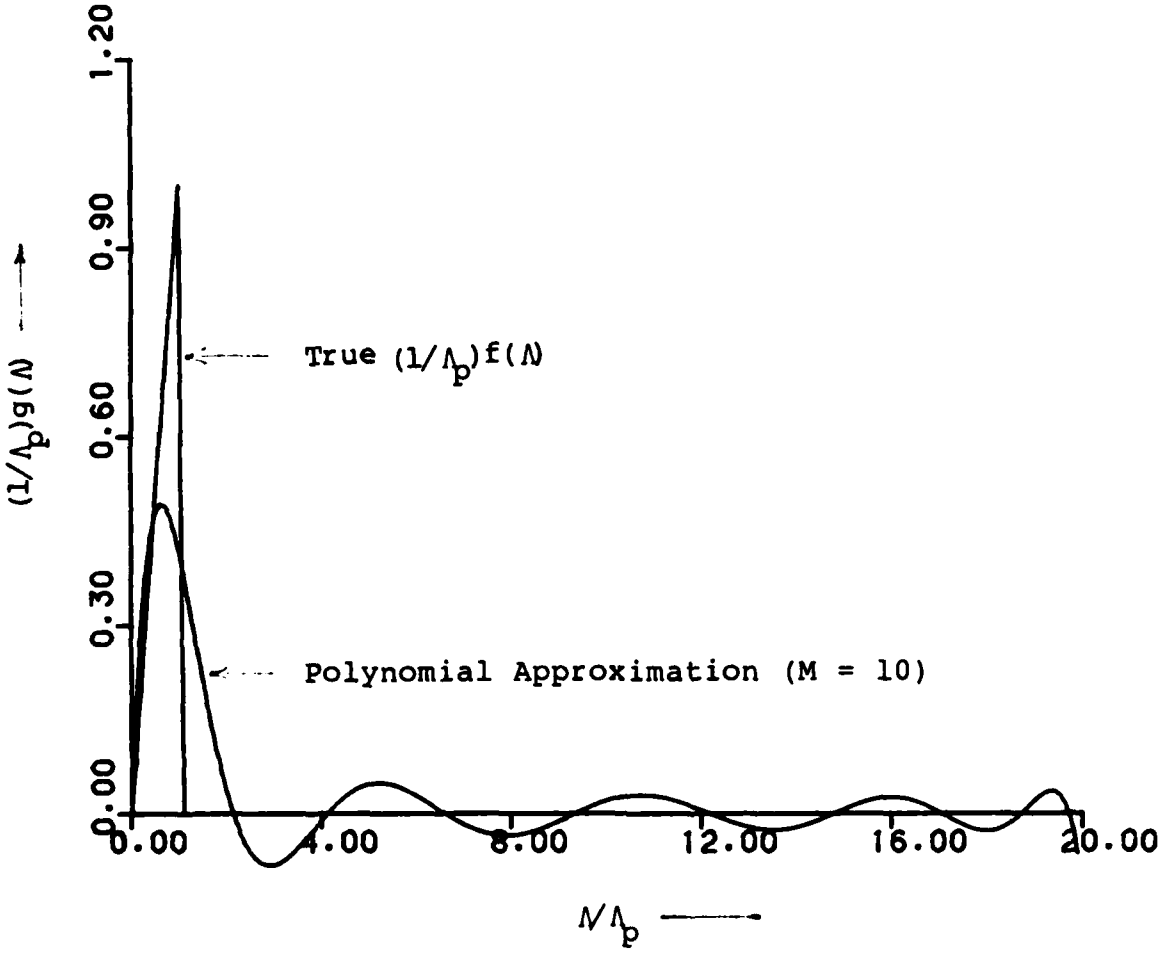

Fig. 2. Polynomial approximation of $f(\Lambda)$. The coefficients of eq. (10) were found for M = 10. The approximation is seen to have negative values for some regions of $\Lambda > \Lambda_p$.

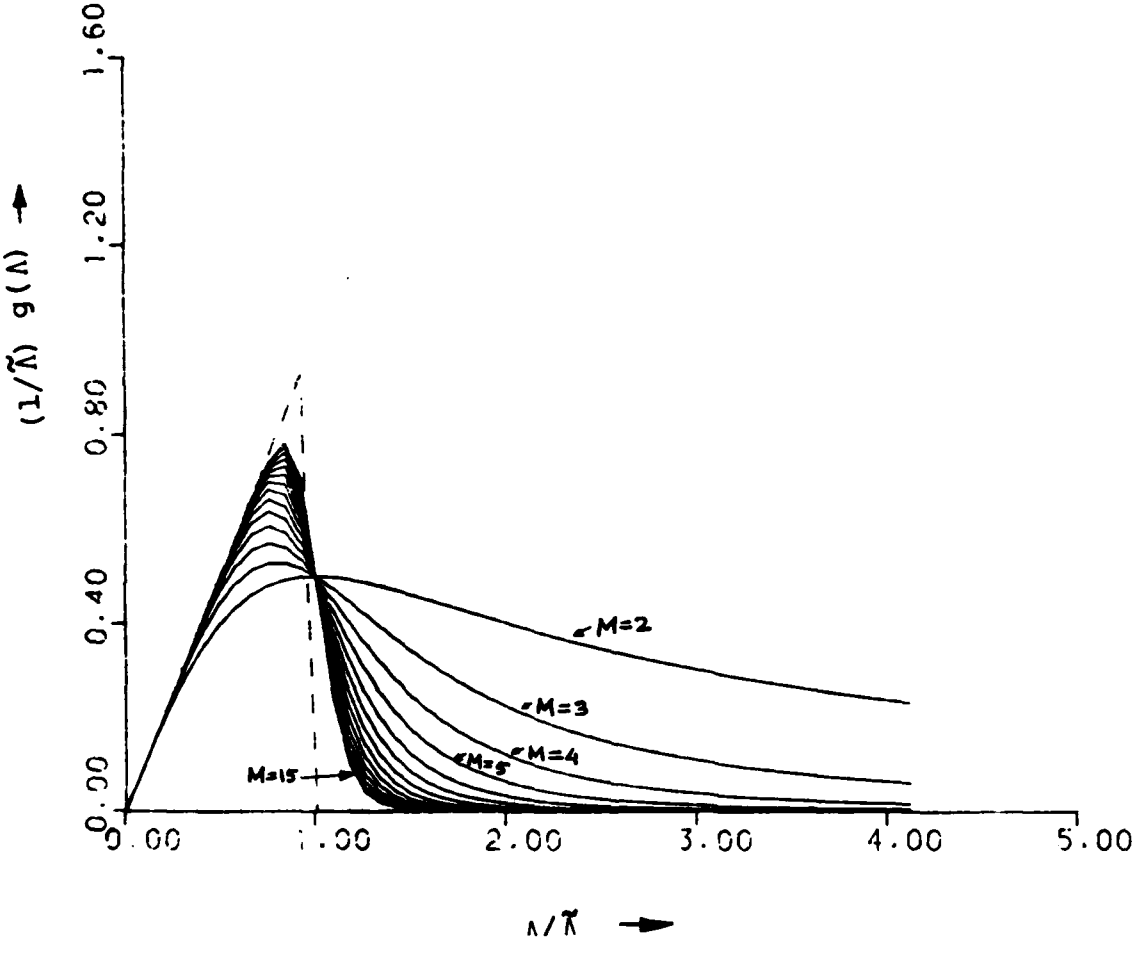

Fig. 3. Rational function approximation of $f(\Lambda)$. Normalized version of $g(\Lambda)$ as in eqn. (12) is shown for M = 2,3, . . ,15.The desired $f(\Lambda)$ is shown by the dotted line. The rational function approx--imation is seen to approach the desired one as M increases.

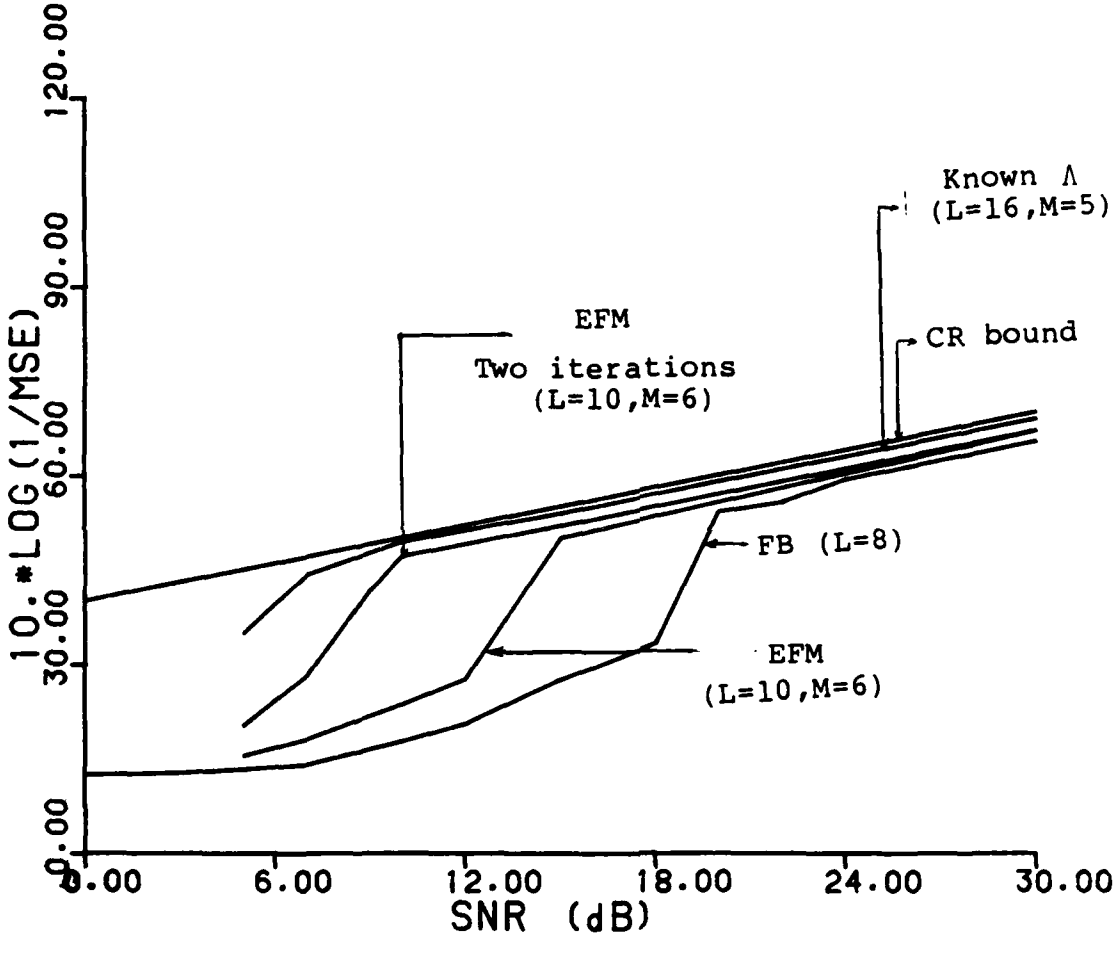

Fig. 4. Performance comparison of the Eigenvalue filtering method with FB method and CR bound. Frequency estimates were chosen from the two zeros of the PEF closest to the unit circle on the z-plane. Plots are shown for the estimate of f_1(=0.52).

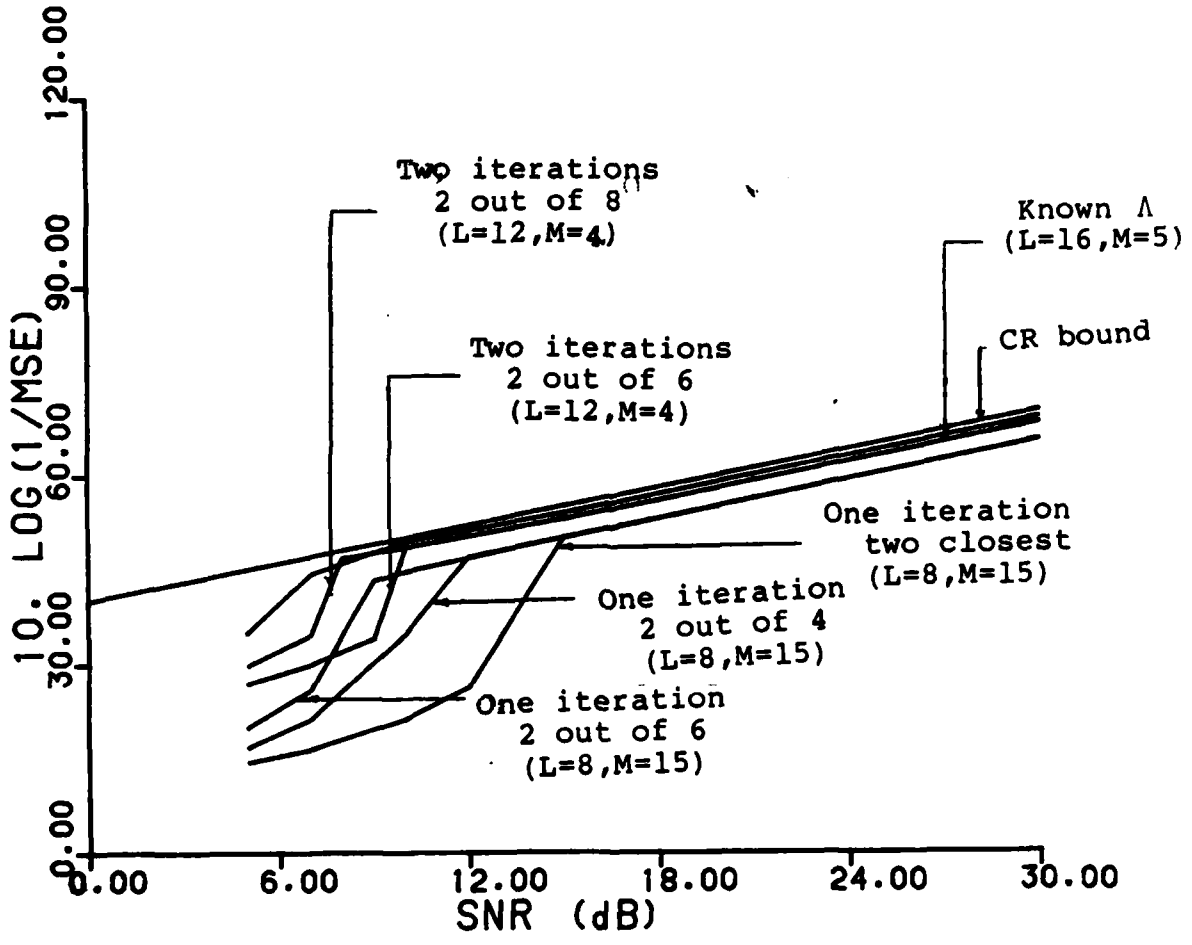

Fig. 5. Performance comparison of the Eigenvalue filtering method with CR bound. The two frequencies having the largest amplitudes were chosen out of 4-8 zeros of the PEF closest to the unit circle on the z-plane. Plots are shown for the estimate of f_1(=0.52).

OFFICE OF NAVAL RESEARCH
STATISTICS AND PROBABILITY PROGRAM

BASIC DISTRIBUTION LIST
FOR
UNCLASSIFIED TECHNICAL REPORTS

FEBRUARY 1982

	Copies
Statistics and Probability Program (Code 411(SP)) Office of Naval Research Arlington, VA 22217	3
Defense Technical Information Center Cameron Station Alexandria, VA 22314	12
Commanding Officer Office of Naval Research Eastern/Central Regional Office Attn: Director for Science Barnes Building 495 Summer Street Boston, MA 02210	1
Commanding Officer Office of Naval Research Western Regional Office Attn: Dr. Richard Lau 1030 East Green Street Pasadena, CA 91101	1
U. S. ONR Liaison Office - Far East Attn: Scientific Director APO San Francisco 96503	1
Applied Mathematics Laboratory David Taylor Naval Ship Research and Development Center Attn: Mr. G. H. Gleissner Bethesda, Maryland 20084	1
Commandant of the Marine Coprs (Code AX) Attn: Dr. A. L. Slafkosky Scientific Advisor Washington, DC 20380	1
Navy Library National Space Technology Laboratory Attn: Navy Librarian Bay St. Louis, MS 39522	1
U. S. Army Research Office P.O. Box 12211 Attn: Dr. J. Chandra Research Triangle Park, NC 27706	1
Director National Security Agency Attn: R51, Dr. Maar Fort Meade, MD 20755	1
ATAA-SL, Library U.S. Army TRADOC Systems Analysis Activity Department of the Army White Sands Missile Range, NM 88002	1
ARI Field Unit-USAREUR Attn: Library c/o ODCSPER HQ USAEREUR & 7th Army APO New York 09403	1
Library, Code 1424 Naval Postgraduate School Monterey, CA 93940	1
Technical Information Division Naval Research Laboratory Washington, DC 20375	1
OASD (I&L), Pentagon Attn: Mr. Charles S. Smith Washington, DC 20301	1

Copies

Director
AMSAA
Attn: DRXSY-MP, H. Cohen
Aberdeen Proving Ground, MD 1
21005

Dr. Gerhard Heiche
Naval Air Systems Command
(NAIR 03)
Jefferson Plaza No. 1
Arlington, VA 20360 1

Dr. Barbara Bailar
Associate Director, Statistical
Standards
Bureau of Census
Washington, DC 20233 1

Leon Slavin
Naval Sea Systems Command
(NSEA 05H)
Crystal Mall #4, Rm. 129
Washington, DC 20036 1

B. E. Clark
RR #2, Box 647-B
Graham, NC 27253 1

Naval Underwater Systems Center
Attn: Dr. Derrill J. Bordelon
Code 601
Newport, Rhode Island 02840 1

Naval Coastal Systems Center
Code 741
Attn: Mr. C. M. Bennett
Panama City, FL 32401 1

Naval Electronic Systems Command
(NELEX 612)
Attn: John Schuster
National Center No. 1
Arlington, VA 20360 1

Defense Logistics Studies
Information Exchange
Army Logistics Management Center
Attn: Mr. J. Dowling
Fort Lee, VA 23801 1

Copies

Reliability Analysis Center (RAC)
RADC/RBRAC
Attn: I. L. Krulac
Data Coordinator/
Government Programs
Griffiss AFB, New York 13441 1

Technical Library
Naval Ordnance Station
Indian Head, MD 20640 1

Library
Naval Ocean Systems Center
San Diego, CA 92152 1

Technical Library
Bureau of Naval Personnel
Department of the Navy
Washington, DC 20370 1

Mr. Dan Leonard
Code 8105
Naval Ocean Systems Center
San Diego, CA 92152 1

Dr. Alan F. Petty
Code 7930
Naval Research Laboratory
Washington, DC 20375 1

Dr. M. J. Fischer
Defense Communications Agency
Defense Communications Engineering
Center
1860 Wiehle Avenue
Reston, VA 22090 1

Mr. Jim Gates
Code 9211
Fleet Material Support Office
U. S. Navy Supply Center
Mechanicsburg, PA 17055 1

Mr. Ted Tupper
Code M-311C
Military Sealift Command
Department of the Navy
Washington, DC 20390 1

	Copies	Copies
Mr. F. R. Del Priori Code 224 Operational Test and Evaluation Force (OPTEVFOR) Norfolk, VA 23511	1	

END

DTIC

9-86